SIAM J. NUMER. ANAL.
Vol. 57, No. 5, pp. 2166–2188

A PERFECTLY MATCHED LAYER APPROACH FOR P_N-APPROXIMATIONS IN RADIATIVE TRANSFER*

HERBERT EGGER† AND MATTHIAS SCHLOTTBOM‡

Abstract. We consider the numerical approximation of boundary conditions in radiative transfer problems by a perfectly matched layer approach. The main idea is to extend the computational domain by an absorbing layer and to use an appropriate reflection boundary condition at the boundary of the extended domain. A careful analysis shows that the consistency error introduced by this approach can be made arbitrarily small by increasing the size of the extension domain or the magnitude of the artificial absorption in the surrounding layer. A particular choice of the reflection boundary condition allows us to circumvent the half-space integrals that arise in the variational treatment of the original vacuum boundary conditions and which destroy the sparse coupling observed in numerical approximation schemes based on truncated spherical harmonics expansions. A combination of the perfectly matched layer approach with a mixed variational formulation and a P_N-finite element approximation leads to discretization schemes with optimal sparsity pattern and provable quasi-optimal convergence properties. As demonstrated in numerical tests these methods are accurate and very efficient for radiative transfer in the scattering regime.

Key words. radiative transfer, perfectly matched layers, Galerkin approximation, P_N method

AMS subject classifications. 65N12, 65N15, 65N30, 65N35

DOI. 10.1137/18M1172521

1. Introduction.

Radiative transfer problems arise in a variety of applications, such as astrophysics, meteorology, nuclear reactor physics, and medical treatment and imaging; we refer to [3, 5, 6, 9, 17, 19] for examples and further references. In this paper, we consider a particular aspect of such models, namely, the efficient numerical treatment of boundary conditions. For ease of presentation, we consider a monochromatic and stationary model problem

$$s \cdot \nabla u(r,s) + \sigma(r) u(r,s) = \int_{\mathcal{S}} k\,(r, s \cdot s')\, u\,(r,s')\, ds' + q(r,s) \quad \text{in } \mathcal{R} \times \mathcal{S}, \tag{1}$$

together with vacuum (homogeneous inflow) boundary conditions

$$u(r,s) = 0 \qquad \text{on } \partial\mathcal{R} \times \mathcal{S} \text{ with } s \cdot n(r) < 0. \tag{2}$$

Here, $n(r)$ is the outer unit normal vector on $\partial\mathcal{R}$. This model describes the transport, absorption, and scattering of particles propagating through a bounded domain $\mathcal{R}$ which is filled by some background medium and surrounded by vacuum. The function $u = u(r,s)$ denotes the density of particles at position $r \in \mathcal{R}$ traveling in direction $s \in \mathcal{S}$, the coefficients $\sigma(r)$ and $k(r, s \cdot s')$ describe the attenuation and scattering properties of the medium, and $q(r,s)$ is a given source density. Due to the inherent tensor product structure of the phase space $\mathcal{R} \times \mathcal{S}$, it seems natural to expand the density $u(r,s)$ into a series

*Received by the editors February 23, 2018; accepted for publication (in revised form) July 11, 2019; published electronically September 5, 2019.
https://doi.org/10.1137/18M1172521
Funding: The work of the authors was supported by 4TU Centre of Competence "Fluid and Solid Mechanics."
†Mathematics, TU Darmstadt, Darmstadt, D-64293 (egger@mathematik.tu-darmstadt.de).
‡Applied Mathematics, University of Twente, Enschede, AE-7500 (m.schlottbom@utwente.nl).

$$u(r,s) = \sum\nolimits_n u_n(r) H_n(s), \tag{3}$$

which allows us to formally recast the radiative transfer equation (1) as an infinite system of coupled partial differential equations for the moments $u_n(r)$. A particularly well-suited choice for the basis functions H_n are the spherical harmonics, since they form a complete orthogonal system in $L^2(\mathcal{S})$ corresponding to the eigenfunctions of the scattering operator. Moreover, the product $sH_n(s)$ can be expressed as a finite combination of spherical harmonics H_m, which leads to a sparse coupling of the moment equations arising from the spherical harmonics expansion; see [3, 16] for details.

In the highly scattering regime, the density $u(r,s)$ can be expected to be a smooth function of s, which results in a fast decay of the moments $u_n(r)$ in the spherical harmonics expansion (3) with $n \to \infty$. A good approximation for the density can thus already be obtained by a truncated series $\sum_{n=0}^{N} u_n(r) H_n(s)$ with N small. Let us note, however, that high smoothness cannot be expected in the vicinity of discontinuities of the material parameters, and, in particular, the solution is typically nonsmooth close to the boundary of the scattering domain. Therefore, a high degree N of the spherical harmonics expansion may be needed to obtain very accurate results. More details of this issue will be discussed in the computational tests.

Inserting the truncated spherical harmonics ansatz into (1) leads to the well-known P_N-approximations, which have been used successfully for theoretical investigations and for the design of numerical approximation schemes; we refer to [5, 9, 20] and [14, 16, 22] for details. While the formal derivation of the P_N-approximation for the radiative transfer equation (1) is rather straightforward, the correct approximation of the vacuum boundary conditions (2) has been subject of controversial discussion for many years; see [17] for a comprehensive overview. A systematic treatment is possible by variational formulations [1, 10, 15], in which the boundary conditions (2) give rise to half-space integrals of the form

$$\int_{\partial\mathcal{R}} \int_{\mathcal{S}:s\cdot n(r)<0} u(r,s) v(r,s) |s \cdot n| \, ds \, dr; \tag{4}$$

here, v denotes the test function in the variational formulation. The appropriate boundary conditions for the P_N-approximation can then be obtained rigorously by Galerkin projection of the underlying variational principle. Let us note that the half-space integrals (4) no longer have a tensor product structure, which actually leads to a dense coupling of almost all moments $u_n(r)$ in the spherical harmonics expansion of the system (1)–(2). Numerical methods based on P_N-approximations, therefore, suffer from a dense coupling of the moment equations originating from the nontensor product structure of the boundary conditions. This not only complicates the implementation but also negatively affects the performance of corresponding discretization methods. In this paper, we propose a strategy to overcome these problems associated with the numerical approximation of the boundary conditions (2). In the spirit of the *perfectly matched layer* (PML) approach, which has been successfully used in the context of acoustic and electromagnetic wave propagation [4, 13], we proceed as follows:

(i) In a first step, the domain $\mathcal{R}$ is extended by an absorbing but nonscattering layer of thickness $\ell > 0$ with absorption coefficient $a > 0$. If vacuum boundary conditions are used at the outer boundary, this yields an equivalent formulation of problem (1)–(2) on an extended domain $\mathcal{R}^\ell$, whose solution $u^{\ell,a}$ coincides with u when restricted to $\mathcal{R}$. Therefore, the solution $u = u^{\ell,a}_{|\mathcal{R}}$ is

in general the restriction of a solution of a radiative transfer equation with discontinuous coefficient functions. Due to the presence of the absorbing layer $\mathcal{R}^\ell \setminus \mathcal{R}$, the solution $u^{\ell,a}$ decays exponentially towards $\partial\mathcal{R}^\ell$.

(ii) In a second step, the vacuum boundary condition at the boundary of the extended domain is replaced by a reflection boundary condition. Since $u^{\ell,a}$ is already small at $\partial\mathcal{R}^\ell$, this introduces a minor perturbation that can be controlled by the absorption parameter a and the thickness ℓ of the absorbing layer in terms of an estimate of the form $\|u^{\ell,a} - w^{\ell,a}\| = O(e^{-\ell a})$, where $w^{\ell,a}$ is the solution of the problem with reflection boundary condition.

An appropriate choice of the thickness ℓ and the absorption coefficient a in the surrounding layer $\mathcal{R}^\ell \setminus \mathcal{R}$ thus allows us to obtain solutions $w^{\ell,a}$ of a perturbed problem, whose restriction to $\mathcal{R}$ approximates the original solution u with any desired accuracy. The rigorous analysis of this approach will be the main topic of the first part of the paper. In the second part of the manuscript, we consider the numerical approximation of the problem with reflection boundary conditions outlined in step (ii). Based on the ideas of [10], we investigate in detail the Galerkin approximation of a mixed variational formulation of the perturbed problem. The possible extension of our analysis to other approaches is briefly discussed at the end of the manuscript. The main new contributions are the following:

(iii) A specific choice of the reflection boundary condition allows us to extend the variational formulation given in [10] to the perturbed problem discussed in step (ii) and to avoid the half-space integrals (4). A careful analysis of the variational problem allows us to establish its well-posedness.

(iv) Under a mild compatibility condition of the approximation spaces, the Galerkin approximation of the mixed variational method leads to discretization schemes with provable convergence properties. A full analysis of the general approach is given, and as a particular example, we discuss in some detail the extension of the P_N-finite element approximation considered in [10, 14, 22]. Due to the absence of the half-space integrals (4), which are eliminated by the particular reflection boundary conditions, the resulting linear systems can be shown to have an optimal sparsity and a tensor product structure that allows for a very efficient solution.

For illustration of theoretical results and in order to demonstrate the efficiency of our approach, we report about some numerical tests for the proposed P_N-finite element approximation with the PML approach at the end of the manuscript. Before we proceed, let us mention a recent paper [18], where the authors considered a somewhat related idea. In this work, a PML approach is used to obtain a problem with periodic boundary conditions in space which in turn can be discretized efficiently by Fourier series. The efficiency of the resulting pseudospectral approximation was illustrated by numerical tests. A full analysis of this approach is not available yet but might be possible with the arguments presented here.

The remainder of the manuscript is organized as follows: In section 2, we introduce our notation and main assumptions, and we recall some preliminary results about well-posedness of the radiative transfer equation. In section 3, we then formulate and analyze the problem in step (i) that arises from extension of the computational domain by an absorbing layer. Section 4 deals with the analysis of the perturbed problem with reflection boundary conditions described in step (ii). In section 5 we consider step (iii) of our approach by deriving a mixed variational formulation of the problem with reflection boundary conditions. In addition, we investigate its systematic Galerkin

approximation and establish rigorous error estimates. In section 6, we address point (iv) by considering an extension of the mixed P_N-finite element method proposed in [10] to the setting considered here. We state a basic compatibility condition of the approximation spaces and discuss some further properties of the method. In section 7, we comment on the efficient implementation of this discretization scheme and then present some numerical tests for illustration of the efficiency of the method. We close with a short discussion and indicate some possible extensions.

2. Preliminaries and notation. Let us start by introducing our notation and basic assumptions that will allow us to guarantee the well-posedness of the radiative transfer problem under consideration. Throughout the manuscript, we make the following assumption.

(A1) The domain $\mathcal{R} \subset \mathbb{R}^3$ is bounded and convex, and we let $\mathcal{S} = \mathcal{S}^2$ be the unit sphere in $\mathbb{R}^3$. The phase space is denoted by $\mathcal{D} = \mathcal{R} \times \mathcal{S}$.

Note that the assumption about convexity of $\mathcal{R}$ is not very restrictive, since one may always extend the domain to a larger ball if required. As usual, we decompose the boundary $\partial\mathcal{D} = \partial\mathcal{R} \times \mathcal{S}$ via

$$\partial\mathcal{D}_\pm = \{(r,s) \in \partial\mathcal{D} : \pm s \cdot n(r) > 0\}$$

into an inflow part $\partial\mathcal{D}_-$ and an outflow part $\partial\mathcal{D}_+$. Let us recall at this point that boundary conditions (2) are required only for the inflow part $\partial\mathcal{D}_-$ of the boundary.

2.1. Function spaces. For any sufficiently regular submanifold $M \subset \mathbb{R}^n$ and any $1 \le p < \infty$, we denote by $L^p(M)$ the usual Lebesgue space of functions on M, and we use $(u,v)_M = \int_M uv\, dM$ to denote the scalar product of $L^2(M)$. Following the notation of [8], we further write

$$W^p(\mathcal{D}) = \{u \in L^p(\mathcal{D}) : s \cdot \nabla u \in L^p(\mathcal{D})\}$$

for the Sobolev space of functions with integrable weak directional derivatives and finite norm given by

$$\|u\|^p_{W^p(\mathcal{D})} = \|u\|^p_{L^p(\mathcal{D})} + \|s \cdot \nabla u\|^p_{L^p(\mathcal{D})}.$$

Let us recall that functions $u \in W^p(\mathcal{D})$ possess well-defined traces on $\partial\mathcal{D}$ in some weighted L^p spaces; see, e.g., [1, 8]. For a.e. $(r,s) \in \partial\mathcal{D}$, we may thus define

$$u_\pm(r,s) = \begin{cases} u(r,s), & \pm s \cdot n(r) > 0, \\ 0 & \text{else.} \end{cases}$$

This induces a natural splitting $u = u_- + u_+$ of the boundary values on $\partial\mathcal{D}$ into an ingoing trace u_- and an outgoing trace u_+, which are, respectively, supported on the corresponding parts $\partial\mathcal{D}_-$ and $\partial\mathcal{D}_+$ of the boundary. By the divergence theorem and a density argument, one can see that

$$(s \cdot \nabla u, v)_{\mathcal{D}} = -(u, s \cdot \nabla v)_{\mathcal{D}} + (s \cdot nu, v)_{\partial\mathcal{D}} \tag{5}$$

holds for all functions u, v with sufficient smoothness and integrability properties. This integration-by-parts formula motivates the definition of weighted trace spaces

$$L^p(\partial\mathcal{D}; |s \cdot n|) = \{g : \partial\mathcal{D} \to \mathbb{R} \quad \text{with} \int_{\partial\mathcal{D}} |g(r,s)|^p |s \cdot n|\, d(r,s) < \infty\},$$

which are strictly smaller than the natural trace spaces of $W^p(\mathcal{D})$; see [1, 8] for details. For any $u \in W^p(\mathcal{D})$ with regular ingoing trace $u_- \in L^p(\partial\mathcal{D}; |s \cdot n|)$, one can deduce from (5) with $v = |u|^{p-2}u$ and some elementary manipulations that

$$\|u_+\|^p_{L^p(\partial\mathcal{D};|s\cdot n|)} = \|u_-\|^p_{L^p(\partial\mathcal{D};|s\cdot n|)} + p\left(s \cdot \nabla u, |u|^{p-2}u\right)_{\mathcal{D}} \le \|u_-\|^p_{L^p(\partial\mathcal{D};|s\cdot n|)} + \|s \cdot \nabla u\|^p_{L^p(\mathcal{D})} + \tfrac{p-1}{p}\|u\|^p_{L^p(\mathcal{D})}. \tag{6}$$

Hence, the norm of the outgoing trace u_+ can be controlled in terms of the norm of the ingoing trace u_- and the norm of the solution u in $W^p(\mathcal{D})$.

2.2. Basic assumptions and well-posedness. In order to ensure the well-posedness of the radiative transfer problem (1)–(2), we will make the following structural assumptions on the model parameters.

(A2) $\sigma \in L^\infty(\mathcal{R})$ with $0 \le \sigma(r) \le \overline{\sigma}$;
(A3) $k : L^\infty(\mathcal{R} \times (-1, 1))$ with $0 \le k(r, \theta) \le \overline{k}$ and $\int_{\mathcal{S}} k(r; s \cdot s')\, ds' \le \sigma(r)$.

These rather general conditions are motivated by physical considerations. The well-posedness of problem (1)–(2) is a special case of the following result, which also covers inhomogeneous boundary conditions.

THEOREM 1. *Let* (A1)–(A3) *hold, and let* $(Ku)(r, s) := \int_{\mathcal{S}} k(r; s \cdot s')u(r, s')\, ds'$ *denote the scattering operator with kernel function* k. *Then, for any* $q \in L^p(\mathcal{D})$ *and any* $g \in L^p(\partial\mathcal{D}; |s \cdot n|)$, *the radiative transfer problem*

$$s \cdot \nabla u + \sigma u = Ku + q \quad \text{in } \mathcal{D}, \tag{7}$$

$$u_- = g_- \quad \text{on } \partial\mathcal{D} \tag{8}$$

has a unique solution $u \in W^p(\mathcal{D})$, *and there holds*

$$\|u\|_{W^p(\mathcal{D})} + \|u_+\|_{L^p(\partial\mathcal{D};|s\cdot n|)} \le C\left(\|q\|_{L^p(\mathcal{D})} + \|g_-\|_{L^p(\partial\mathcal{D};|s\cdot n|)}\right)$$

with constant C depending only on $\overline{\sigma}$ and $\operatorname{diam}(\mathcal{R})$.

Proof. Existence of a unique solution and the bound for u in the norm of $W^p(\mathcal{D})$ follow from [11, Theorem 1.1 and Theorem 8.3]. The remaining estimate for the outgoing trace u_+ can then be deduced from (6). ∎

Note that problem (1)–(2) is just a special case of (7)–(8) with $g_- = 0$. Under assumptions (A1)–(A3), the model problem (1)–(2) is therefore well-posed.

Part 1. The perfectly matched layer approach.

In the following two sections, we investigate the approximation of (1)–(2) by radiative transfer problems on larger domains. We start with an equivalent problem and then introduce a perturbation by incorporating a reflection boundary condition.

3. Equivalent problems on larger domains. Problem (1)–(2) describes the propagation of particles through a domain $\mathcal{R}$ surrounded by vacuum. We will now show that the domain $\mathcal{R}$ can also be embedded in an absorbing medium without changing the solution. For any $r \in \mathbb{R}^d \setminus \mathcal{R}$ and $s \in \mathcal{S}$, we denote by

$$\ell(r, s) = \inf\{l > 0 : r - ls \in \mathcal{R}\} \tag{9}$$

the distance of the point r to the boundary $\partial\mathcal{R}$ of the computational domain along the path with direction $-s$ starting at r; see Figure 1. Using standard convention, we

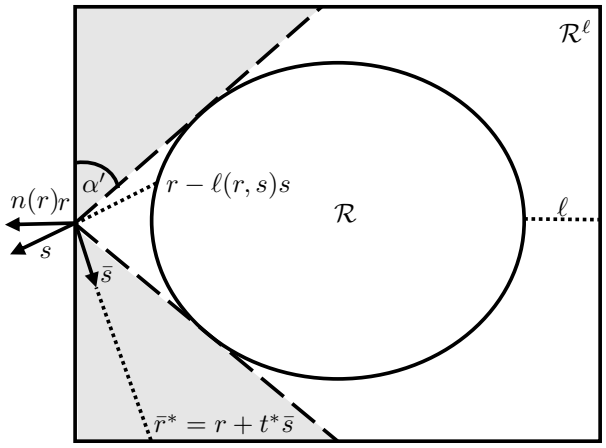

FIG. 1. *Sketch of the geometric setup for two spatial dimensions. $\mathcal{R}$ corresponds to the disc. The extended domain $\mathcal{R}^\ell$ corresponds to the bounding rectangle. The distance between $\partial\mathcal{R}$ and $\partial\mathcal{R}^\ell$ is given by ℓ, and the point (r,s) is an element of the outflow boundary $\partial\mathcal{D}^\ell_+$ of the layer such that $\ell(r,s) < \infty$, i.e., $r - \ell(r,s)s \in \partial\mathcal{R}$. Moreover, we have that $s \cdot n(r) \geq \sin(\alpha')$. On the other hand, lines through r that pass through the gray area do not intersect $\mathcal{R}$. For instance, the path $t \mapsto r + t\bar{s}$, $t \in \mathbb{R}$, does not intersect $\mathcal{R}$. Moreover, there exists a unique $t^* > 0$ such that $r^* = r + t^*\bar{s} \in \partial\mathcal{R}^\ell$ and $(r^*, \bar{s}) \in \partial\mathcal{D}^\ell_+$, which will become important for the construction of the reflection boundary conditions described in step* (ii).

set $\ell(r,s) = \infty$ if the corresponding path does not intersect the boundary $\partial\mathcal{R}$. We then consider extensions $\mathcal{R}^\ell$ of the domain $\mathcal{R}$ with the following properties.

(A4) For given $\ell, \eta > 0$, let $\mathcal{R}^\ell \subset \mathbb{R}^3$ be a bounded convex domain with $\overline{\mathcal{R}} \subset \mathcal{R}^\ell$ compactly embedded and such that $\ell(r,s) \geq \ell$ for a.e. $(r,s) \in \partial\mathcal{D}^\ell = \partial\mathcal{R}^\ell \times \mathcal{S}$ and $\ell(r,s) = \infty$ for a.e. $(r,s) \in \partial\mathcal{D}^\ell$ with $s \cdot n(r) \leq \eta =: \sin\alpha$.

Remark 2. Note that $\ell \leq \operatorname{dist}\{\partial\mathcal{R}^\ell, \mathcal{R}\}$ is a lower bound on the thickness of the extension layer $\widetilde{\mathcal{R}} = \mathcal{R}^\ell \setminus \mathcal{R}$. Moreover, $0 < \eta = \sin\alpha$ yields a lower bound on the angles α' at which beams originating from points $r \in \mathcal{R}$ can hit the boundary $\partial\mathcal{R}^\ell$ and lines in direction s going through points $r \in \mathcal{R}^\ell \setminus \mathcal{R}$ with $\ell(r,s) = \ell(r,-s) = \infty$ do not intersect the domain $\mathcal{R}$; see Figure 1 for illustration. These geometric properties will become important for our analysis below.

As a next step, we extend the definition of the model parameters to $\mathcal{R}^\ell$ by

$$\begin{aligned} &\sigma^{\ell,a}(r) = \sigma(r), \quad k^\ell(r,\cdot) = k(r,\cdot), \quad q^\ell(r,\cdot) = q(r,\cdot), \qquad r \in \mathcal{R}, \\ &\sigma^{\ell,a}(r) = a, \qquad k^\ell(r,\cdot) = 0, \qquad q^\ell(r,\cdot) = 0, \qquad r \in \mathcal{R}^\ell \setminus \mathcal{R}, \end{aligned}$$

and we denote by K^ℓ the scattering operator associated to the kernel k^ℓ. The choice $a = 0$ means that $\mathcal{R}$ is surrounded by vacuum, while $a > 0$ models the case that the original domain is embedded in an absorbing but nonscattering medium. On the extended domain $\mathcal{D}^\ell = \mathcal{R}^\ell \times \mathcal{S}$, we then consider the problem

$$s \cdot \nabla u^{\ell,a} + \sigma^{\ell,a} u^{\ell,a} = K^\ell u^{\ell,a} + q^\ell \quad \text{on } \mathcal{D}^\ell, \tag{10}$$

$$u^{\ell,a}_- = 0 \quad \text{on } \partial\mathcal{D}^\ell. \tag{11}$$

With the same arguments as used for the proof of Theorem 1, one can again obtain the existence of a unique solution. Due to the particular definition of the parameters in the extension layer, we obtain some further properties of the solution.

THEOREM 3. *Let* (A1)–(A4) *hold and* $a \geq 0$. *Then for any* $q \in L^p(\mathcal{D})$, *the extended problem* (10)–(11) *has a unique solution* $u^{\ell,a} \in W^p(\mathcal{D}^\ell)$, *which can be represented as* $u^{\ell,a} = E^{\ell,a}u$, *where* u *is the solution of* (1)–(2) *and where the extension operator* $E^{\ell,a}$ *is defined by*

$$(E^{\ell,a}u)(r,s) = \begin{cases} u(r,s), & (r,s) \in \mathcal{D}, \\ e^{-a\ell(r,s)}u(r-\ell(r,s)s,s), & (r,s) \in \mathcal{D}^\ell \setminus \mathcal{D},\ 0 < \ell(r,s) < \infty, \\ 0, & \text{else.} \end{cases}$$

Moreover, $u^{\ell,a}|_{\mathcal{D}} = u$ *and* $u^{\ell,a}(r,s) = 0$ *for* $(r,s) \in \partial\mathcal{D}^\ell$ *with* $\ell(r,s) = \infty$, *and*

$$\|u^{\ell,a}\|_{L^p(\partial\mathcal{D}^\ell)} \leq Ce^{-a\ell}\|q\|_{L^p(\mathcal{D})} \tag{12}$$

with constant C *depending only on* $\overline{\sigma}$, $\operatorname{diam}(\mathcal{R})$, *and the constant* η *in* (A4).

Proof. Existence of a unique solution $u^{\ell,a}$ follows from [11, Theorem 1.1 and Theorem 8.3]. The remaining assertions are proven by the following lemma. ∎

LEMMA 4. *Let* (A1)–(A4) *hold, and let* $u \in W^p(\mathcal{D})$ *with* $u_- = 0$ *on* $\partial\mathcal{D}$. *Then for any* $a \geq 0$, *we have* $E^{\ell,a}u \in W^p(\mathcal{D}^\ell)$ *and*

$$\|s \cdot \nabla E^{\ell,a}u\|_{L^p(\mathcal{D}^\ell\setminus\mathcal{D})} = a\|E^{a,\ell}u\|_{L^p(\mathcal{D}^\ell\setminus\mathcal{D})} \leq a^{1-\frac{1}{p}}\|u\|_{W^p(\mathcal{D})}.$$

Moreover, $(E^{\ell,a}u)(r,s) = 0$ *for any* $(r,s) \in \partial\mathcal{D}^\ell$ *with* $\ell(r,s) = \infty$, *and, therefore,*

$$\begin{aligned} \eta^{1/p}\|E^{\ell,a}u\|_{L^p(\partial\mathcal{D}^\ell)} &\leq \|E^{\ell,a}u\|_{L^p(\partial\mathcal{D}^\ell;|s\cdot n|)} \\ &\leq e^{-a\ell}\|u_+\|_{L^p(\partial\mathcal{D};|s\cdot n|)} \leq e^{-a\ell}\|u\|_{W^p(\mathcal{D})}. \end{aligned}$$

Proof. By construction, $\widetilde{u} = (E^{\ell,a}u)|_{\widetilde{\mathcal{D}}}$, with $\widetilde{\mathcal{D}} = \mathcal{D}^\ell \setminus \mathcal{D}$, is a solution to

$$s \cdot \nabla\widetilde{u} + a\widetilde{u} = 0 \quad \text{in } \widetilde{\mathcal{D}}, \tag{13}$$

$$\widetilde{u}_- = u_+ \quad \text{on } \partial\widetilde{\mathcal{D}} \cap \partial\mathcal{D} \quad \text{and} \quad \widetilde{u}_- = 0 \quad \text{on } \partial\widetilde{\mathcal{D}} \cap \partial\mathcal{D}^\ell. \tag{14}$$

Note that the normal vector pointing out of the layer $\widetilde{\mathcal{R}} = \mathcal{R}^\ell \setminus \mathcal{R}$ has to be used in the definition of $\widetilde{u}_\pm$, while that pointing out of $\mathcal{R}$ is used in the definition of $u_\pm$. From [11, Theorem 1.2] with $\nu = 1$, $\sigma = a$, and $f = 0$ and noting that $s \cdot \nabla\widetilde{u} = -a\widetilde{u}$, we infer that $\widetilde{u} \in W^p(\widetilde{\mathcal{D}})$ and

$$\|s \cdot \nabla\widetilde{u}\|_{L^p(\widetilde{\mathcal{D}})} = a\|\widetilde{u}\|_{L^p(\widetilde{\mathcal{D}})} \leq a^{1-\frac{1}{p}}\|u_+\|_{L^p(\partial\mathcal{D};|s\cdot n|)}.$$

From (6) and $u_- = 0$ on $\partial\mathcal{D}$, we deduce that

$$\|u_+\|_{L^p(\partial\mathcal{D};|s\cdot n|)} \leq \|u\|_{W^p(\mathcal{D})}, \tag{15}$$

which proves the first estimate.Moreover, we have $\widetilde{u}_+ = 0 = u_-$, and, by (14), $\widetilde{u}_- = u_+$ on $\partial\mathcal{D}$. Hence $\widetilde{u} = u$ on $\partial\mathcal{D}$, which shows that $E^{\ell,a}u$ is continuous across $\partial\mathcal{D}$ in the sense of traces. Together with $(E^{\ell,a}u)|_{\mathcal{D}} = u \in W^p(\mathcal{D})$ and $(E^{\ell,a}u)|_{\widetilde{\mathcal{D}}} = \widetilde{u} \in W^p(\widetilde{\mathcal{D}})$, this implies that $E^{\ell,a}u \in W^p(\mathcal{D}^\ell)$; see [1, Remark 2.5]. By the definition of the extension and condition (A4), one can see that $E^{\ell,a}u(r,s) = 0$ for all $(r,s) \in \partial\mathcal{D}^\ell$ with $\ell(r,s) = \infty$; cf. Figure 1. In addition, one can infer that $|E^{\ell,a}u(r,s)| \leq$

$e^{-a\ell}|E^{\ell,0}u(r,s)|$ on $\partial\widetilde{\mathcal{D}}$. But since $s\cdot\nabla E^{\ell,0}u = 0$ on $\widetilde{\mathcal{D}}$ and $(E^{\ell,0}u)_+ = 0$ on $\partial\widetilde{\mathcal{D}}\cap\partial\mathcal{D}$ by construction, we may deduce from (6), with $\mathcal{D}$ replaced by $\widetilde{\mathcal{D}}$, that

$$\|E^{\ell,0}u\|_{L^p(\partial\mathcal{D}^\ell;|s\cdot n|)} \overset{(14)}{=} \left\|\left(E^{\ell,0}u\right)_+\right\|_{L^p\left(\partial\widetilde{\mathcal{D}};|s\cdot n|\right)} \overset{(6)}{=} \left\|\left(E^{\ell,0}u\right)_-\right\|_{L^p(\partial\widetilde{\mathcal{D}};|s\cdot n|)}$$
$$\overset{(14)}{=} \left\|\left(E^{\ell,0}u\right)_-\right\|_{L^p(\partial\widetilde{\mathcal{D}}\cap\partial\mathcal{D};|s\cdot n|)} = \|u_+\|_{L^p(\partial\mathcal{D};|s\cdot n|)}.$$

In the last step, we used the continuity of $E^{\ell,0}u$ across $\partial\mathcal{D}$ and the fact that the normal vectors at $\partial\widetilde{\mathcal{R}}\cap\partial\mathcal{R}$ and $\partial\mathcal{R}$ have opposite sign. Using (15) and $(E^{\ell,a}u)(r,s) = 0$ for all $(r,s)\in\partial\mathcal{D}^\ell$ with $s\cdot n(r)\le\eta$, we obtain the second estimate of the lemma. ∎

Remark 5. An important consequence of Theorem 3 is that the trace of the solution $u^{\ell,a}$ of the extended problem (10)–(11) is an element of $L^p(\partial\mathcal{D}^\ell)$ without weight, i.e., it has somewhat higher regularity. This is due to the geometric setting and the purely absorbing but nonscattering behavior of the surrounding layer and will be important for our further considerations:

4. A modified boundary condition. The estimate (12) implies that the solution $u^{\ell,a}$ can be made arbitrarily small at the outer boundary $\partial\mathcal{D}^\ell$ by choosing the parameters a,ℓ sufficiently large. A perturbation of the boundary condition at $\partial\mathcal{D}^\ell$ should, therefore, only have a minor effect. As approximation for (10)–(11), we thus consider in this section the following problem with modified boundary conditions:

$$s\cdot\nabla w^{\ell,a} + \sigma^{\ell,a}w^{\ell,a} = K^\ell w^{\ell,a} + q^\ell \quad \text{in } \mathcal{D}^\ell, \tag{16}$$
$$w^{\ell,a}_- = Rw^{\ell,a}_+ \quad \text{on } \partial\mathcal{D}^\ell, \tag{17}$$

where $R : L^p(\partial\mathcal{D}^\ell;|s\cdot n|)\to L^p(\partial\mathcal{D}^\ell;|s\cdot n|)$ is an appropriate reflection operator. Motivated by the considerations of section 5, we here consider the particular choice

$$(Rg)(r,s) = \frac{s\cdot n+1}{s\cdot n-1}g_+(r,-s), \qquad (r,s)\in\partial\mathcal{D}^\ell. \tag{18}$$

Particles arriving in direction $-s$ at the boundary $\partial\mathcal{D}^\ell$, thus, partially leave the domain or get, otherwise, reflected in the opposite direction s. In the analysis of this section, we will only make use of the following properties.

LEMMA 6. *The operator $R : L^p(\partial\mathcal{D}^\ell;|s\cdot n|)\to L^p(\partial\mathcal{D}^\ell;|s\cdot n|)$ is linear, and $Rg = (Rg)_-$. Moreover, $|Rg(r,s)|\le|g(r,-s)|$ for a.e. $(r,s)\in\partial\mathcal{D}^\ell_-$. If* (A4) *holds, then $|Rg(r,s)|\le(1-\eta)|g(r,-s)|$ if $\ell(r,-s)<\infty$.*

Proof. The validity of the assertions follows directly from the definition (18). ∎

4.1. Well-posedness of the perturbed problem. We will now show by a contraction argument that problem (16)–(18) admits a unique solution. The key ingredient is that most particles that leave the domain $\mathcal{R}$ get absorbed before they arrive at the reflection boundary $\partial\mathcal{R}^\ell$. Moreover, points $(r,s)\in\mathcal{D}^\ell$ with $\ell(r,s)=\infty$ cannot be reached by particles originating from the domain $\mathcal{R}$. Let us denote by

$$H_- = \{h_-\in L^p(\partial\mathcal{D}^\ell;|s\cdot n|) : h_-(r,s) = 0 \text{ if } \ell(r,-s)=\infty\} \tag{19}$$

the space of inflow boundary values at $\partial\mathcal{D}^\ell$ which corresponds to particles that may hit the computational domain $\mathcal{R}$ after travelling along straight lines through the extension layer $\mathcal{R}^\ell\setminus\mathcal{R}$. The following result is essential for our contraction argument.

LEMMA 7. *Let* (A1)–(A4) *hold. Then for any* $q \in L^p(\mathcal{D})$ *and* $h_- \in H_-$*, the problem*

$$s \cdot \nabla z^{\ell,a} + \sigma^{\ell,a} z^{\ell,a} = K^\ell z^{\ell,a} + q^\ell \quad \text{in } \mathcal{D}^\ell, \tag{20}$$

$$z_-^{\ell,a} = h_- \quad \text{on } \partial\mathcal{D}^\ell \tag{21}$$

has a unique solution $z^{\ell,a} \in W^p(\mathcal{D}^\ell)$*, and* $z_+^{\ell,a}(r,s) = 0$ *for a.e. point* $(r,s) \in \partial\mathcal{D}^\ell$ *with* $\ell(r,s) = \infty$*. Moreover, there holds*

$$\left\| z^{\ell,a} \right\|_{W^p(\mathcal{D})} \le C \left(\|q\|_{L^p(\mathcal{D})} + e^{-a\ell} \|h_-\|_{L^p(\partial\mathcal{D}^\ell;|s\cdot n|)} \right)$$

with constant C *depending only on* $\overline{\sigma}$ *and* $\operatorname{diam}(\mathcal{R})$*. In addition,*

$$\left\| z_+^{\ell,a} \right\|_{L^p(\partial\mathcal{D}^\ell;|s\cdot n|)}^p \le e^{-pa\ell} \left(e^{-pa\ell} \|h_-\|_{L^p(\partial\mathcal{D}^\ell;|s\cdot n|)}^p + p\|q\|_{L^p(\mathcal{D})} \left\| z^{\ell,a} \right\|_{L^p(\mathcal{D})}^{p-1} \right).$$

Proof. Existence of a unique solution $z^{\ell,a} \in W^p(\mathcal{D}^\ell)$ follows with the same arguments as in Theorem 1. Now let $\widetilde{\mathcal{D}} = \mathcal{D}^\ell \setminus \mathcal{D}$ denote the extension layer. Then due to the linearity of the problem, we can decompose $z^{\ell,a}$ on $\widetilde{\mathcal{D}}$ as $z^{\ell,a} = \widetilde{z}^a + E^{\ell,a} z$, where $z = z^{\ell,a}|_{\mathcal{D}}$ and $\widetilde{z}^a$ is the solution of the auxiliary problem

$$\begin{aligned} s \cdot \nabla \widetilde{z}^a + a\widetilde{z}^a &= 0 \qquad \text{in } \widetilde{\mathcal{D}}, \\ \widetilde{z}_-^a &= h_- \quad \text{on } \partial\widetilde{\mathcal{D}}_- \cap \partial\mathcal{D}^\ell \quad \text{and} \quad \widetilde{z}_-^a = 0 \quad \text{on } \partial\widetilde{\mathcal{D}}_- \cap \partial\mathcal{D}. \end{aligned}$$

With similar arguments as in the proof of Lemma 4, one can show that

$$\begin{aligned} \|\widetilde{z}^a\|_{L^p(\partial\mathcal{D};|s\cdot n|)} &= \left\| \widetilde{z}_+^a \right\|_{L^p\left(\partial\widetilde{\mathcal{D}}\cap\partial\mathcal{D};|s\cdot n|\right)} \\ &\le e^{-a\ell} \left\| \widetilde{z}_+^0 \right\|_{L^p\left(\partial\widetilde{\mathcal{D}}\cap\partial\mathcal{D};|s\cdot n|\right)} \le e^{-a\ell} \|h_-\|_{L^p(\partial\mathcal{D}^\ell;|s\cdot n|)}. \end{aligned}$$

In the last step, we used the a priori estimate of Theorem 1 for the problem defining the solution $\widetilde{z}^a$ with $a = 0$. From the decomposition $z^{\ell,a} = \widetilde{z}^a + E^{\ell,a} z$, the definition of $z = z^{\ell,a}|_{\mathcal{D}}$, and the continuity of $z^{\ell,a}$ across $\partial\mathcal{D}$, we deduce that

$$z_- = \widetilde{z}_+^a \qquad \text{on } \partial\widetilde{\mathcal{D}} \cap \partial\mathcal{D},$$

i.e., the particles entering $\mathcal{D}$ via $\partial\mathcal{D}$ are those generated by h_- on $\partial\mathcal{D}^\ell$ and leaving the surrounding layer $\widetilde{\mathcal{D}} = \mathcal{D}^\ell \setminus \mathcal{D}$ via $\partial\mathcal{D}$. The function $z = z^{\ell,a}|_{\mathcal{D}}$ hence solves

$$\begin{aligned} s \cdot \nabla z + \sigma z &= Kz + q \quad \text{in } \mathcal{D}, \\ z_- &= g_- \qquad \text{on } \partial\mathcal{D} \end{aligned}$$

with boundary data $g_- = \widetilde{z}_+^a$. From Theorem 1 and the previous estimates, we get

$$\left\| z^{\ell,a} \right\|_{W^p(\mathcal{D})} = \|z\|_{W^p(\mathcal{D})} \le C' \left(\|q\|_{L^p(\mathcal{D})} + e^{-a\ell} \|h_-\|_{L^p(\partial\mathcal{D}^\ell;|s\cdot n|)} \right).$$

The additional bound for the outgoing trace $z_+^{\ell,a} = E^{\ell,a} z$ can then be deduced from the second estimate of Theorem 1 and Lemma 4. ∎

We are now in the position to establish the well-posedness of problem (16)–(18).

THEOREM 8. *Let* (A1)–(A4) *hold. Then, for any* $q \in L^p(\mathcal{D})$ *and any* $a > 0$*, problem* (16)–(17) *has a unique solution* $w^{\ell,a} \in W^p(\mathcal{D}^\ell)$ *with*

$$\left\| w^{\ell,a} \right\|_{W^p(\mathcal{D})} \le C\|q\|_{L^p(\mathcal{D})} \quad \text{and} \quad \left\| w^{\ell,a} \right\|_{L^p(\partial\mathcal{D}^\ell)} \le Ce^{-a\ell}\|q\|_{L^p(\mathcal{D})}$$

with constant C *depending only on* $\overline{\sigma}$*,* $\operatorname{diam}(\mathcal{R})$*, and* η*.*

Proof. In a first step, we show that for any solution $w^{\ell,a} \in W^p(\mathcal{D}^\ell)$ there holds

$$w^{\ell,a}(r,s) = 0 \qquad \text{for a.e. } (r,s) \in \partial\mathcal{D}^\ell \text{ with } \ell(r,s) = \ell(r,-s) = \infty, \tag{22}$$

which implies that $w^{\ell,a} \equiv 0$ on the union of all lines that do not intersect the computational domain $\mathcal{R}$; cf. Remark 2. Let (r,s) be such a point on the outer boundary $\partial\mathcal{D}_-^\ell$ with $\ell(r,s) = \ell(r,-s) = \infty$. Then $r + ts \in \mathcal{R}^\ell \setminus \mathcal{R}$ for all $0 < t < t^*$, where t^* is chosen such that $r^* = r + t^*s \in \partial\mathcal{R}^\ell$; see Figure 1. Since the medium in the extension layer $\mathcal{R}^\ell \setminus \mathcal{R}$ is purely absorbing, we have $w^{\ell,a}(r + ts, s) = e^{-at} w^{\ell,a}(r,s)$. Applying the reflection operator at the point (r^*, s), we further obtain

$$\left|w^{\ell,a}(r^*,-s)\right| = \left|Rw^{\ell,a}(r^*,-s)\right| \le \left|w^{\ell,a}(r^*,s)\right| = e^{-at^*}\left|w^{\ell,a}(r,s)\right|.$$

Repeating the argument with $r = r^* - t^*s$ yields $|w^{\ell,a}(r,s)| \le e^{-2at^*}|w^{\ell,a}(r,s)|$, which implies that $w^{\ell,a}(r,s) = 0$ and shows the assertion (22).

As a consequence, we know that any solution $w^{\ell,a} \in W^p(\mathcal{D})$ has to satisfy $w^{\ell,a}|_{\partial\mathcal{D}_-^\ell} = h_- \in H_-$ as in (19). We now show the existence and uniqueness of such a solution. For any given $h_- \in H_-$, we define $\Phi(h_-) := Rz_+$, where $z \in W^p(\mathcal{D}^\ell)$ is the unique solution of

$$s \cdot \nabla z + \sigma^{\ell,a} z = K^\ell z + q^\ell \quad \text{in } \mathcal{D}^\ell, \tag{23}$$

$$z_- = h_- \quad \text{on } \partial\mathcal{D}^\ell. \tag{24}$$

The results of Lemma 7 imply that $z_+(r,s) = 0$ for $(r,s) \in \partial\mathcal{D}^\ell$ with $\ell(r,s) = \infty$, and thus $Rz_+ \in H_-$ by Lemma 6. Hence $\Phi : H_- \to H_-$ is a self-mapping on the nonempty and closed subset H_- of the Banach space $L^p(\partial\mathcal{D}^\ell; |s \cdot n|)$. By taking the difference of two solutions z, z' with boundary data $h_-, h'_- \in H_-$, we further deduce from Lemma 6 and Lemma 7 that

$$\begin{aligned}\|\Phi(h_-) - \Phi(h'_-)\|_{L^p(\partial\mathcal{D}^\ell;|s\cdot n|)} &= \|Rz_+ - Rz'_+\|_{L^p(\partial\mathcal{D}^\ell;|s\cdot n|)} \\ &\le (1-\eta)\|z_+ - z'_+\|_{L^p(\partial\mathcal{D}^\ell;|s\cdot n|)} \le (1-\eta)e^{-2a\ell}\|h_- - h'_-\|_{L^p(\partial\mathcal{D};|s\cdot n|)}.\end{aligned}$$

This shows that Φ is a contraction on H_- and by Banach's fixed-point theorem, there exists a unique fixed point $h_- \in H_-$ with $\Phi(h_-) = h_-$. By construction, the function $w^{\ell,a} = z$ with z as defined above then is the unique solution of (16)–(17). Now set $h_-^0 = 0$ and for $n \ge 1$ define $h_-^n = \Phi(h_-^{n-1})$. Then from the convergence estimates for Banach's fixed-point iteration, we obtain

$$\|h_-\|_{L^p(\partial\mathcal{D}^\ell;|s\cdot n|)} = \left\|h_- - h_-^0\right\|_{L^p(\partial\mathcal{D}^\ell;|s\cdot n|)} \le \frac{1}{1-\eta}\left\|h_-^1 - h_-^0\right\|_{L^p(\partial\mathcal{D}^\ell;|s\cdot n|)}.$$

Due to the choice $h_-^0 = 0$, we know that $h_-^1 = Ru^{\ell,a}$, where $u^{\ell,a}$ is the unique solution of (10)–(11). From Lemma 6 and the estimate (12), we can then deduce that

$$\begin{aligned}\eta^{1/p}\|h_-\|_{L^p(\partial\mathcal{D}^\ell)} &\le \|h_-\|_{L^p(\partial\mathcal{D}^\ell;|s\cdot n|)} \\ &\le \frac{1}{1-\eta}\left\|u_+^{\ell,a}\right\|_{L^p(\partial\mathcal{D}^\ell;|s\cdot n|)} \le \frac{C}{1-\eta}e^{-a\ell}\|q\|_{L^p(\mathcal{D})}.\end{aligned}$$

From the construction of h_-, one can see that the solution $w^{\ell,a} = z$ of the auxiliary problem (23)–(24) is the unique solution of problem (16)–(17). The proof is thus completed by an application of Lemma 7, which yields the bounds for the solution. ∎

4.2. Error estimates. In preparation of the next theorem, let us state a bound for the solution $w^{\ell,a}$ of the perturbed problem on the extension layer.

LEMMA 9. *Let* (A1)–(A4) *hold and* $w^{\ell,a}$ *be the solution of* (16)–(17)*. Then*

$$\big\|s\cdot\nabla w^{\ell,a}\big\|_{L^p(\mathcal{D}^\ell\setminus\mathcal{D})} + a\,\big\|w^{\ell,a}\big\|_{L^p(\mathcal{D}^\ell\setminus\mathcal{D})} \le Ca^{\frac{p-1}{p}}\|q\|_{L^p(\mathcal{D})}$$

with constant C *depending only on* $\bar\sigma$, $\operatorname{diam}(\mathcal{R})$, *and* η.

Proof. Observe that $w^{\ell,a}$ is a solution to

$$\begin{aligned} s\cdot\nabla w^{\ell,a} + aw^{\ell,a} &= 0 && \text{in } \widetilde{\mathcal{D}},\\ w_-^{\ell,a} &= (w^{\ell,a}|_{\mathcal{D}})_+ && \text{on } \partial\widetilde{\mathcal{D}}\cap\partial\mathcal{D},\\ w_-^{\ell,a} &= Rw^{\ell,a} && \text{on } \partial\widetilde{\mathcal{D}}\cap\partial\mathcal{D}^\ell. \end{aligned}$$

In view of Theorem 8, we already know that

$$\begin{aligned} \big\|w_+^{\ell,a}\big\|_{L^p(\partial\mathcal{D};|s\cdot n|)} &\le C\,\big\|w^{\ell,a}\big\|_{W^p(\mathcal{D})} \le C\|q\|_{L^p(\mathcal{D})} \qquad \text{and}\\ \big\|Rw^{\ell,a}\big\|_{L^p(\mathcal{D}^\ell;|s\cdot n|)} &\le \big\|w^{\ell,a}\big\|_{L^p(\mathcal{D}^\ell;|s\cdot n|)} \le Ce^{-a\ell}\|q\|_{L^p(\mathcal{D})}. \end{aligned}$$

The assertion now follows with the same arguments as in the proof of Lemma 4. ∎

In combination with the previous results, we can now derive explicit estimates for the perturbation error resulting from the use of the reflection boundary condition.

THEOREM 10. *Let* (A1)–(A4) *hold, and let* u *and* $w^{\ell,a}$ *denote the solutions of problem* (1)–(2) *and of problem* (16)–(17)*, respectively. Then*

$$\big\|w^{\ell,a}-u\big\|_{W^p(\mathcal{D})} \le Ce^{-2a\ell}\|q\|_{L^p(\mathcal{D})}$$

with constant C *depending only on* $\bar\sigma$, $\operatorname{diam}(\mathcal{R})$, *and* η. *Moreover,*

$$\big\|s\cdot\nabla\big(w^{\ell,a}-E^{\ell,a}u\big)\big\|_{L^p(\mathcal{D}^\ell\setminus\mathcal{D})} + a\,\big\|\big(w^{\ell,a}-E^{\ell,a}u\big)\big\|_{L^p(\mathcal{D}^\ell\setminus\mathcal{D})} \le Ca^{\frac{p-1}{p}}e^{-a\ell}\|q\|_{L^p(\mathcal{D})}.$$

Proof. By Theorem 3, we have $u = u^{\ell,a}|_{\mathcal{D}}$, where $u^{\ell,a}$ is the solution of (10)–(11). The difference $z^{\ell,a} = w^{\ell,a} - u^{\ell,a}$ satisfies (20)–(21) with $h_- = Rw^{\ell,a}$ and $q^\ell = 0$. The first bound then follows by a combination of Lemma 6, Lemma 7, and Theorem 8, and the second estimate follows similarly using Lemma 9. ∎

Remark 11. As shown in [11] the constant C in Theorem 1 is uniformly bounded for all $1 \le p \le \infty$. Using the basic fact that, on bounded domains, the L^∞-norm of an essentially bounded function can be obtained as the limit $p\to\infty$ of its corresponding L^p-norms, the results of the first part generalize to the case $p=\infty$ directly.

Part 2. Numerical approximation.

In the following two sections, we discuss the numerical approximation of problem (16)–(17) by extending the mixed variational approach proposed in [10]. We first derive a variational formulation of the problem and consider its systematic Galerkin approximation, and then we discuss a particular method based on a tensor product approximation using spherical harmonics and mixed finite elements.

5. A mixed variational problem. For ease of notation, we write $w = w^{\ell,a}$ and $q = q^\ell$ in the following and consider the problem

$$s \cdot \nabla w + \sigma^{\ell,a} w = K^\ell w + q \quad \text{in } \mathcal{D}^\ell, \tag{25}$$

$$w_- = R w_+ \qquad \text{on } \partial\mathcal{D}^\ell. \tag{26}$$

As before, the reflection operator is defined by $(Rg)(r,s) = \frac{s\cdot n+1}{s\cdot n-1} g_+(r,-s)$, and the particular form will become important now. Based on the derivation of the perturbed problem, we know that $q \equiv 0$ and $k^\ell \equiv 0$ in the extension layer $\partial\mathcal{R}^\ell \setminus \mathcal{R}$.

5.1. Even-odd splitting. Following [10], we start with the splitting of functions $v(r,s)$ into even and odd parts with respect to direction s defined by

$$v^\pm(r,s) = \frac{1}{2}\left(v(r,s) \pm v(r,-s)\right). \tag{27}$$

Let us note that the splitting $v = v^+ + v^-$ is orthogonal with respect to the scalar product of $L^2(\mathcal{S})$. This allows us to rewrite the problem (25)–(26) as follows.

LEMMA 12. *Let $w \in W^2(\mathcal{D}^\ell)$ denote a solution of problem (25)–(26). Then*

$$s \cdot \nabla w^- + \sigma^{\ell,a} w^+ = K^\ell w^+ + q^+ \quad \textit{in } \mathcal{D}^\ell, \tag{28}$$

$$s \cdot \nabla w^+ + \sigma^{\ell,a} w^- = K^\ell w^- + q^- \quad \textit{in } \mathcal{D}^\ell, \tag{29}$$

$$w^+ = s \cdot n w^- \qquad \textit{on } \partial\mathcal{D}. \tag{30}$$

If, on the other hand, $w^\pm \in W^2(\mathcal{D}^\ell)$ solve (28)–(30), then $w = w^+ + w^- \in W^2(\mathcal{D}^\ell)$ is a solution of (25)–(26). The two problems are thus equivalent in this sense.

Proof. Let us note that multiplication with σ and application of K^ℓ preserves parity, i.e., these operations map even to even and odd to odd functions, while application of $s \cdot \nabla$ reverts the parity. Together with the orthogonality of the splitting (27) this already shows the equivalence of (25) and (28)–(29). Using the definition of the reflection operator, the boundary condition (26) can be rewritten as

$$(1 - s\cdot n) w(r,s) = -(1 + s \cdot n) w(r,-s) \qquad \text{for } (r,s) \in \partial\mathcal{D}^\ell_-.$$

A reordering of the terms and inserting the definition of $w^\pm$ further yields

$$\begin{aligned} 2w^+(r,s) &= w(r,s) + w(r,-s) \\ &= s\cdot n[w(r,s) - w(r,-s)] = 2s\cdot n w^-(r,s) \qquad \text{for } (r,s) \in \partial\mathcal{D}^\ell_-, \end{aligned}$$

which shows that (30) is valid on $\partial\mathcal{D}_-$. Now note that the left- and right-hand side of the last identity each define even functions of s. This shows that (30) also holds on $\partial\mathcal{D}^\ell_+$. The equivalence of (26) with (30) follows by reverting the arguments. ∎

5.2. Variational characterization. We can now use the equivalent formulation (28)–(30) to derive a weak form of problem (25)–(26). The function spaces

$$\mathbb{W}^+ = \left\{u^+ \in W^2\left(\mathcal{D}^\ell\right) : u^+|_{\partial\mathcal{D}^\ell} \in L^2\left(\partial\mathcal{D}^\ell\right)\right\} \qquad \text{and} \qquad \mathbb{V}^\pm = \left\{u^\pm \in L^2\left(\mathcal{D}^\ell\right)\right\}$$

turn out to be appropriate for representing the even and odd solution components of the problem under investigation. The tensor product space $\mathbb{W}^+ \times \mathbb{V}^-$ is equipped with its natural norm given by

$$\left|\!\left|\!\left| \left(u^+, u^-\right) \right|\!\right|\!\right|^2 = \left\|s\cdot\nabla u^+\right\|^2_{L^2(\mathcal{D}^\ell)} + \left\|u^+\right\|_{L^2(\partial\mathcal{D}^\ell)} + \left\|u^+\right\|^2_{L^2(\mathcal{D}^\ell)} + \left\|u^-\right\|^2_{L^2(\mathcal{D}^\ell)}. \tag{31}$$

For ease of notation, we further define the total collision operator

$$\mathcal{C} : L^2(\mathcal{D}^\ell) \to L^2(\mathcal{D}^\ell), \quad v \mapsto \sigma^{\ell,a} v - K^\ell v.$$

We then obtain the following variational characterization of solutions.

LEMMA 13. *Let $w \in W^2(\mathcal{D}^\ell)$ denote a solution of problem (25)–(26) or, equivalently, of problem (28)–(30). Then for all $v^+ \in \mathbb{W}^+$ and $v^- \in \mathbb{V}^-$ there holds*

$$(w^+, v^+)_{\partial\mathcal{D}^\ell} + (\mathcal{C}w^+, v^+)_{\mathcal{D}^\ell} - (w^-, s\cdot\nabla v^+)_{\mathcal{D}^\ell} = (q^+, v^+)_{\mathcal{D}^\ell}, \tag{32}$$

$$(s\cdot\nabla w^+, v^-)_{\mathcal{D}^\ell} + (\mathcal{C}w^-, v^-)_{\mathcal{D}^\ell} = (q^-, v^-)_{\mathcal{D}^\ell}. \tag{33}$$

Proof. Recall that $(u,v)_M = \int_M uv dM$ denotes the scalar product of $L^2(M)$. Multiplying (28) with a test function $v^+ \in \mathbb{W}^+$ and integrating over $\mathcal{D}^\ell$ yields

$$(q^+ - \mathcal{C}w^+, v^+)_{\mathcal{D}^\ell} = (s\cdot\nabla w^-, v^+)_{\mathcal{D}^\ell} = -(w^-, s\cdot\nabla v^+)_{\mathcal{D}^\ell} + (s\cdot n w^-, v^+)_{\partial\mathcal{D}^\ell}.$$

Here, we made use of the integration-by-parts formula (5) in the last step. The boundary condition (30) allows us to replace the last term, and inserting the definition of the collision operator $\mathcal{C}$ then already yields (32). The validity of (33) follows immediately by testing (29) with $v^- \in \mathbb{V}^-$. ∎

Let us note at this point that, due to the particular reflection boundary condition, no half-space integrals appear in the variational characterization of the perturbed problem.

5.3. Weak formulation. We can now give the following weak formulation of problem (25)–(26) and of the equivalent problem (28)–(30), respectively.

PROBLEM 14. *Find $w^+ \in \mathbb{W}^+$ and $w^- \in \mathbb{V}^-$ such that (32)–(33) holds.*

Let us note that existence of a weak solution is immediately obtained from Theorem 8 and Lemma 13. To show uniqueness and to facilitate the further discussion, we will make the following assumption in what follows.

(A5) $\gamma\|v\|^2_{L^2(\mathcal{D}^\ell)} \le (\mathcal{C}v, v)_{\mathcal{D}^\ell} \le \Gamma\|v\|_{L^2(\mathcal{D}^\ell)}$ for all $v \in L^2(\mathcal{D}^\ell)$ for some $0 < \gamma, \Gamma$.

This condition is valid, e.g., if the medium is uniformly absorbing, and it implies that the artificial absorption has to satisfy $\gamma \le a \le \Gamma$ as well. Using the arguments of [10, section 3.3], the assumption could be further relaxed. Due to (A5) the total collision operator $\mathcal{C} : L^2(\mathcal{D}^\ell) \to L^2(\mathcal{D}^\ell)$ is boundedly invertible, which allows us to define norms

$$\|u\|^2_{\mathcal{C}} = (\mathcal{C}u, u)_{\mathcal{D}^\ell} \qquad \text{and} \qquad \|u\|^2_{\mathcal{C}^{-1}} = (\mathcal{C}^{-1}u, u)_{\mathcal{D}^\ell},$$

which are equivalent to the norm on $L^2(\mathcal{D}^\ell)$, i.e., $\gamma\|u\|^2_{L^2(\mathcal{D}^\ell)} \le \|u\|^2_{\mathcal{C}} \le \Gamma\|u\|^2_{L^2(\mathcal{D}^\ell)}$ and $\Gamma^{-1}\|u\|^2_{L^2(\mathcal{D}^\ell)} \le \|u\|^2_{\mathcal{C}^{-1}} \le \gamma^{-1}\|u\|^2_{L^2(\mathcal{D}^\ell)}$. By minor modification of the arguments used in [10], we can now deduce the following assertion.

THEOREM 15. *Let (A1)–(A5) hold. Then problem (32)–(33) has a unique solution $w^+ \in \mathbb{W}^+$ and $w^- \in \mathbb{V}^-$, and there holds*

$$|||(w^+, w^-)||| \le C_D \|q\|_{L^2(\mathcal{D})}$$

with constant C_D depending at most linearly on γ^{-1} and Γ. In addition, the function $w = w^+ + w^- \in W^2(\mathcal{D}^\ell)$ coincides with the unique solution of (25)–(26).

Proof. The proof of [10, Theorem 3.1] applies almost verbatim and yields the existence and uniqueness of a solution as well as the a priori estimate

$$\|s\cdot\nabla u^+\|^2_{\mathcal{C}^{-1}} + \|u^+\|^2_{\mathcal{C}} + \|u^+\|^2_{L^2(\partial\mathcal{D}^\ell)} + \|u^-\|^2_{\mathcal{C}} \le C\|q\|^2_{\mathcal{C}^{-1}}$$

with a universal constant $C > 0$. Let us note that the change of the boundary term does not affect the proof given in [10]. The postulated bounds for the solution then follow using assumption (A5) and the equivalence of the norms $\|\cdot\|_{\mathcal{C}}$, $\|\cdot\|_{\mathcal{C}^{-1}}$, and $\|\cdot\|_{L^2(\mathcal{D}^\ell)}$. The last assertion follows by the uniqueness of the weak solution and noting that, according to Lemma 13, the solution of (25)–(26) also solves (32)–(33). ∎

5.4. Galerkin approximation. Let $\mathbb{W}^+_h \subset \mathbb{W}^+$ and $\mathbb{V}^-_h \subset \mathbb{V}^-$ be closed subspaces. We then consider the following Galerkin approximation of Problem 14.

PROBLEM 16. *Find* $(w^+_h, w^-_h) \in \mathbb{W}^+_h \times \mathbb{V}^-_h$ *such that*

$$(\mathcal{C}w^+_h, v^+_h)_{\mathcal{D}^\ell} + (w^+_h, v^+_h)_{\partial\mathcal{D}^\ell} - (w^-_h, s\cdot\nabla v^+_h)_{\mathcal{D}^\ell} = (q^+, v^+_h)_{\mathcal{D}^\ell} \qquad \forall v^+_h \in \mathbb{W}^+_h, \tag{34}$$

$$(s\cdot\nabla w^+_h, v^-_h)_{\mathcal{D}^\ell} + (\mathcal{C}w^-_h, v^-_h)_{\mathcal{D}^\ell} = (q^-, v^-_h)_{\mathcal{D}^\ell} \qquad \forall v^-_h \in \mathbb{V}^-_h. \tag{35}$$

In order to ensure the existence of a unique discrete solution, we require the following.

(A6) $\mathbb{W}^+_h \subset \mathbb{W}^+$, $\mathbb{V}^-_h \subset \mathbb{V}^-$ are finite dimensional and $\{s\cdot\nabla w^+_h : w^+_h \in \mathbb{W}^+_h\} \subset \mathbb{V}^-_h$.

This condition guarantees the uniform stability of the discrete variational problem. By the same arguments as used in [10, section 6], we then obtain the following results.

LEMMA 17. *Let assumptions* (A1)–(A6) *be valid. Then Problem* 16 *has a unique solution* $(w^+_h, w^-_h) \in \mathbb{W}^+_h \times \mathbb{V}^-_h$, *and*

$$|||(w^+_h, w^-_h)||| \le C_D\|q\|_{L^2(\mathcal{D})}$$

with the same constant C_D *as in Theorem* 15. *Moreover,*

$$|||(w^+ - w^+_h, w^- - w^-_h)||| \le C'_D \inf |||(w^+ - v^+_h, w^- - v^-_h)|||,$$

where the infimum is taken over all $(v^+_h, v^-_h) \in \mathbb{W}^+_h \times \mathbb{V}^-_h$. *The constant* C'_D *again depends at most linearly on* γ^{-1} *and* Γ.

Proof. The assertions result from application of the Babuška–Aziz lemma. Details can be found in the proof of [10, Theorem 6.1]. ∎

Together with the results of section 4, we finally obtain the following error estimate.

THEOREM 18. *Let* (A1)–(A6) *hold, and let* u, $w = w^{\ell,a}$, *and* (w^+_h, w^-_h) *denote the unique solutions of* (1)–(2), *of* (25)–(26), *and of Problem* 16, *respectively. Then*

$$\begin{aligned}\|u^+ - w^+_h\|_{W^2(\mathcal{D})} + \|u^- - w^-_h\|_{L^2(\mathcal{D})} &\\ \le C_D e^{-a\ell}\|q\|_{L^2(\mathcal{D})} + C'_D \inf |||(w^+ - v^+_h, w^- - v^-_h)|||.&\end{aligned}$$

The infimum is again taken over all $(v^+_h, v^-_h) \in \mathbb{W}^+_h \times \mathbb{V}^-_h$, *and the constants* C_D *and* C'_D *depend at most linearly on* γ^{-1} *and* Γ.

Proof. The result follows from the previous results via the triangle inequality. ∎

Remark 19. The approximation error in the above theorem involves the function w, which itself depends on the PML parameters ℓ and a. For uniformly bounded parameters a, ℓ, we can, however, expect convergence with $N \to \infty$ and $h \to 0$. Let

us assume for simplicity that the best-approximation error can be bounded uniformly in a and ℓ by $\inf |||(w^+ - v_h^+, w^- - v_h^-)||| = O(h)$. Then the optimal choice of the parameters ℓ, a would be such that $e^{-\ell a} \approx h$, where we neglect the at most linear dependence of C_D' on a. Hence, it suffices to choose a or ℓ proportional to $|\log h|$ in order to obtain a quasi-optimal overall approximation. We expect that such a mild variation in the parameters will only have a small effect on the regularity of the function w, which has to be approximated; see Table 3 and Figure 3 for a numerical illustration. Let us also note that, in view of Theorem 10, $\inf |||(w^+ - v_h^+, w^- - v_h^-)|||$ can replaced by $\inf |||(E^{\ell,a}u^+ - v_h^+, E^{\ell,a}u^- - v_h^-)|||$ in the estimate of Theorem 18, which can be possibly made explicit under regularity assumptions on the solution u of the original problem.

6. The P_N-finite element method. We now discuss a particular construction of approximation spaces $\mathbb{W}_h^+$ and $\mathbb{V}_h^-$ using spherical harmonics and finite elements.

6.1. Angular approximation. As angular basis functions H_n in the moment expansion (3), we employ the spherical harmonics Y_l^m, $-l \le m \le l$, $l \ge 0$ in the sequel. These functions form an orthonormal basis for $L^2(\mathcal{S})$ and allow us to efficiently realize the splitting (27), since Y_{2l}^m and Y_{2l+1}^m are even and odd functions, respectively. For the approximation of even and odd functions of angular variable s, we then consider the spaces

$$\mathbb{S}_N^+ = \operatorname{span}\{Y_{2l}^m, 0 \le 2l \le N, -2l \le m \le 2l\},$$
$$\mathbb{S}_N^- = \operatorname{span}\{Y_{2l+1}^m, 0 \le 2l+1 \le N, -2l-1 \le m \le 2l+1\}.$$

Let us note that $\dim(\mathbb{S}_N^\pm) \approx N^2$. We will later only consider the choice N odd; necessary modifications for the case N even can be found in [10].

6.2. Spatial approximation. We denote by $\mathcal{T}_h = \mathcal{T}_h(\mathcal{R}^\ell)$ a quasi-uniform regular partition of the spatial domains $\mathcal{R}^\ell \subset \mathbb{R}^3$ into simplicial elements T of size h and assume that $\mathcal{T}_h(\mathcal{R}) = \{T \in \mathcal{T}_h(\mathcal{R}^\ell) : T \subset \overline{\mathcal{R}}\}$ is a conforming mesh of the original domain $\mathcal{R} \subset \mathcal{R}^\ell$. By $\mathcal{P}_k(\mathcal{T}_h) = \{v \in L^2(\mathcal{R}^\ell) : v|_T \in P_k(T)\}$, we denote the spaces of piecewise polynomials over $\mathcal{T}_h$ of degree less or equal to k. For the approximation of the even and odd moments u_n in the expansion (3), we utilize the spaces

$$\mathbb{X}_h^+ = \mathcal{P}_1(\mathcal{T}_h) \cap H^1(\mathcal{R}^\ell) \qquad \text{and} \qquad \mathbb{X}_h^- = \mathcal{P}_0(\mathcal{T}_h) \subset L^2(\mathcal{R}^\ell).$$

We denote by $\{\varphi_j\}$ and $\{\chi_k\}$ the canonical basis consisting of hat functions and piecewise constant functions, respectively, and recall that $\dim(\mathbb{X}_h^+) \approx \dim(\mathbb{X}_h^-) \approx h^{-3}$.

6.3. Tensor product spaces. As choice for the spaces $\mathbb{W}_h^+$ and $\mathbb{V}_h^-$ in Problem 16, we then consider the following tensor product construction:

$$\mathbb{W}_h^+ = \mathbb{X}_h^+ \otimes \mathbb{S}_N^+ \quad \text{and} \quad \mathbb{V}_h^- = \mathbb{X}_h^- \otimes \mathbb{S}_N^-.$$

By similar arguments as in [10, 22], one can show the following properties.

LEMMA 20. *Let $\mathbb{W}_h^+$ and $\mathbb{V}_h^-$ be as above. Then $\dim(\mathbb{W}_h^+) \approx \dim(\mathbb{V}_h^-) \approx h^{-3}N^2$. If N is chosen odd, then assumption* (A6) *is satisfied.*

Proof. The estimates for the dimensions are obtained directly from the tensor product construction. By well-known recurrence relations for spherical harmonics, one can further see that sY_l^m is of the form [3, 22]

$$sY_l^m = \begin{pmatrix} a_{1lm}Y_{l-1}^{m-1} + b_{2lm}Y_{l-1}^{m+1} + c_{3lm}Y_{l+1}^{m-1} + d_{4lm}Y_{l+1}^{m+1} \\ a_{1lm}Y_{l-1}^{m-1} + b_{2lm}Y_{l-1}^{m+1} + c_{3lm}Y_{l+1}^{m-1} + d_{4lm}Y_{l+1}^{m+1} \\ e_{lm}Y_{l-1}^m + f_{lm}Y_{l+1}^m \end{pmatrix}.$$

Together with the assumption that N is odd, this implies that $s\mathbb{S}_N^+ \subset (\mathbb{S}_N^-)^3$. Since the derivative of a continuous piecewise linear function is piecewise constant, we further have $\nabla \mathbb{X}_h^+ \subset (\mathbb{X}_h^-)^3$. The compatibility condition in (A6) then follows directly from the tensor product construction. ∎

As a consequence of the previous lemma, all results presented in section 5 apply directly to the P_N-finite element method based on this choice of approximation spaces.

6.4. Complexity estimates. The choice of a basis for $\mathbb{W}_h^+$ and $\mathbb{V}_h^-$ allows us to recast the discrete variational problem (34)–(35) as a linear system,

$$\begin{aligned} \mathtt{M}\mathtt{w}^+ + \mathtt{R}\mathtt{w}^+ - \mathtt{B}^\top \mathtt{w}^- &= \mathtt{q}^+, \\ \mathtt{B}\mathtt{w}^+ + \mathtt{C}\mathtt{w}^- &= \mathtt{q}^-, \end{aligned}$$

where $\mathtt{w}^+$, $\mathtt{w}^-$, $\mathtt{q}^+$, $\mathtt{q}^-$ are the corresponding coefficient vectors. When choosing the natural tensor product basis with components $\{\varphi_j Y_{2m}^l\}$ for the even components and $\{\chi_j Y_{2m+1}^l\}$ for the odd components, the resulting system matrices can be seen to have some favorable properties.

LEMMA 21. *Let assumptions* (A2)–(A3) *and* (A5)–(A6) *hold and* $a > 0$. *Then the matrices* $\mathtt{M}$ *and* $\mathtt{C}$ *are symmetric and positive definite, and* $\mathtt{R}$ *is symmetric and positive semidefinite. If the basis for* $\mathbb{W}_h^+$ *and* $\mathbb{V}_h^-$ *are chosen as described above, then* $\mathtt{M}$ *and* $\mathtt{R}$ *are block-diagonal with sparse blocks,* $\mathtt{B}$ *is block-sparse with sparse blocks, and* $\mathtt{C}$ *is diagonal. Moreover, the number of nonzero entries is given by* $nnz(\mathtt{M}) \approx nnz(\mathtt{B}) \approx nnz(\mathtt{C}) \approx h^{-3}N^2$ *and* $nnz(\mathtt{R}) \approx h^{-2}N^2$.

As a direct consequence of these properties, the multiplication with any of the system matrices can be achieved in order optimal complexity.

Remark 22. In our numerical tests, we consider test problems with symmetries. For instance, in section 7.2 we consider a two-dimensional cross-section $\mathcal{R} \subset \mathbb{R}^2$ of the three-dimensional domain while the angular domain still is $\mathcal{S} = \mathbb{S}^2$. In that case, the spatial mesh $\mathcal{T}_h$ consists of triangles and $\dim(\mathbb{X}_h^\pm) \approx h^{-2}$, and consequently $\dim(\mathbb{W}_h^+) \approx \dim(\mathbb{V}_h^-) \approx h^{-2}N^2$. All observations made above apply with obvious modifications also to such settings.

6.5. Solution of the linear system. Let us finally also comment briefly on the efficient solution of the linear system arising from the tensor-product P_N-finite element approximation. Since the matrix $\mathtt{C}$ is diagonal and positive definite, one can eliminate $\mathtt{w}^-$ via the second equation by

$$\mathtt{w}^- = \mathtt{C}^{-1}(\mathtt{q}^- - \mathtt{B}\mathtt{w}^+). \tag{36}$$

Note that $\mathtt{w}^-$ can be computed efficiently once the even component $\mathtt{w}^+$ of the solution is known. Inserting the formula for $\mathtt{w}^-$ into the first equation yields the Schur complement system

$$[\mathtt{M} + \mathtt{R} + \mathtt{B}^\top \mathtt{C}^{-1}\mathtt{B}]\mathtt{w}^+ = \mathtt{q}^+ + \mathtt{B}^\top \mathtt{C}^{-1}\mathtt{q}^-. \tag{37}$$

Using Lemma 21, the matrix $\mathtt{S} = [\mathtt{M} + \mathtt{R} + \mathtt{B}^\top \mathtt{C}^{-1}\mathtt{B}]$ is symmetric and positive definite. Moreover, the matrix vector product $\mathtt{S} \cdot \mathtt{w}^+$ can be realized, even without assembling $\mathtt{S}$, with $h^{-3}N^2$ algebraic operations and thus in optimal complexity. For the efficient numerical solution of the Schur complement system, we can employ a preconditioned conjugate gradient (PCG) method. In our numerical tests, we utilize a spatial multigrid strategy for preconditioning, cf. [2, 7].

7. Numerical illustrations. We now illustrate the theoretical results obtained in the previous sections by numerical tests, which model physically realistic three-dimensional problems that can be described by reduced models due to symmetries.

7.1. Slab geometry. We consider the spatial domain $\mathcal{R} = \mathbb{R}^2 \times (0,1)$ and assume that all functions only depend on the third coordinate z and on the azimuthal angle of the direction s via $\mu = \cos\theta$. In this setting, the radiative transfer equation with isotropic scattering reduces to

$$\mu \partial_z u(z,\mu) + \sigma(z) u(z,\mu) = \frac{\sigma_s}{2} \int_{-1}^{1} u(z,\mu') d\mu' + q(z,\mu), \tag{38}$$

which is assumed to hold for all (z,μ) in the slab $\mathcal{D} = (0,1) \times (-1,1)$. In addition, we assume homogeneous inflow boundary conditions, which here read

$$u(0,\mu) = 0 \quad \text{and} \quad u(1,-\mu) = 0 \qquad \text{for} \quad 0 < \mu < 1. \tag{39}$$

Let us recall that this quasi-one-dimensional setting, usually called slab geometry, amounts to a three-dimensional problem with particular symmetries [5].

For discretization of the radiative transfer problem (38)–(39), we use a mixed P_N-finite element approximation outlined in the previous section. The spherical harmonics are given here by $H_n(\mu) = P_n(\mu)$, where P_n denotes the nth Legendre polynomial. As in multiple dimensions, the even moments in the expansion are approximated by continuous piecewise linear finite elements over a mesh of the spatial domain, and the odd moments are approximated by piecewise constant functions.

For our computational tests, we set the parameters to $\sigma_s = 1$ and $\sigma = 1.01$, which corresponds to a scattering dominated regime. The source density is chosen as $q(z,\mu) = \exp(-100(z-0.5)^2)$. Snapshots of the reference solution for problem (38)–(39) obtained with our numerical methods with $N = 1001$ moments and $nz = 1024$ elements are depicted in Figure 2.

Let us note that the solutions seem almost indistinguishable, which is in perfect agreement with the estimates of Theorem 18. In the following, we investigate the behavior of the error

$$\big(\|u_h - w_h^{a,\ell}\|^2_{L^2(\mathcal{D})} + \|\mu \partial_z (u_h^+ - w_h^{a,\ell,+})\|^2_{L^2(\mathcal{D})} \big)^{1/2} \tag{40}$$

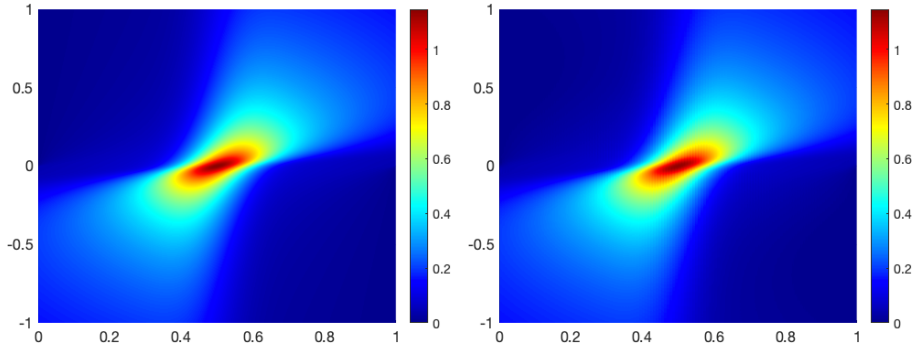

FIG. 2. *Numerical solutions as functions of* $0 < z < 1$ *and* $-1 < \mu < 1$ *for slab geometry with* $N = 1001$ *moments,* $nz = 1024$ *mesh elements, and standard boundary conditions (left) and approximation with* $N = 101$ *moments,* $nz = 128$ *mesh elements, and PML treatment of the boundary condition with* $a = 3$ *and* $\ell = 0.15$ *(right).*

TABLE 1

Observed errors $\|u_h - w_h^{a,\ell}\|$ between finite element solution u_h with standard boundary condition and the solution $w_h^{a,\ell}$ based on the PML approach with parameters a and ℓ of the layer with norm as in (40). In both cases, the discretization parameters were chosen as $N = 1001$ and $nz = 512$.

	ℓ				
a	0.0	0.1	0.2	0.3	0.4
1.0	0.1084	0.0687	0.0456	0.0308	0.0214
2.0	0.1084	0.0456	0.0215	0.0107	0.0056
3.0	0.1084	0.0310	0.0108	0.0041	0.0017
4.0	0.1084	0.0215	0.0057	0.0017	0.0006
5.0	0.1084	0.0152	0.0031	0.0007	0.0003

TABLE 2

Observed errors $|||w^{a,\ell} - w_{N,h}^{a,\ell}|||$ for the finite element solutions in dependence of the discretization parameters for the mixed problem with PML boundary conditions with $a = 3$ and $\ell = 0.2$.

	N				
nz	21	41	81	161	321
64	0.0407	0.0181	0.0133	0.0131	0.0131
128	0.0391	0.0141	0.0071	0.0067	0.0067
256	0.0387	0.0129	0.0043	0.0034	0.0033
512	0.0386	0.0126	0.0032	0.0018	0.0016

in dependence of the two terms in the right-hand side of the corresponding error estimate in more detail.

In Table 1, we display the errors introduced by the numerical handling of the boundary conditions via the PML approach for different model parameters a and ℓ. As predicted by the estimates of Theorem 10, we can observe exponential convergence in both model parameters, i.e., in the thickness ℓ and in the absorption coefficient a of the PML layer. In fact, as expected, the relevant parameter is $a\ell$. The error to the reference solution is $\|u - u_h\| = 0.001$, which shows that the consistency errors introduced by the PML approach can be made small compared to the approximation errors that result from the finite element discretization. Let us also note that much smaller errors are obtained with respect to the zero order moment, which contains the most valuable information in practice.

As a next step, we study in more detail the approximation error estimates stated in Lemma 17 and Theorem 18. In Table 2, we display the errors in the numerical solution measured in the norm $|||\cdot|||$ defined in (31). As a reference solution, we choose the one obtained with the same methods but the finest discretization with $N = 1001$ moments and $nz = 1024$ mesh elements.

For any fixed number of moments N, we observe convergence $O(h)$ with respect to the mesh size $h = 1/nz$, until saturation occurs due to the error of the truncated moment approximation. Vice versa, we also observe convergence with respect to N until saturation due to the spatial approximation occurs. The overall convergence behavior can be expected in view of the results of Theorem 18, since for fixed PML parameters a, ℓ, the function $w = w^{\ell,a}$ in the estimate does not change.

The overall convergence behavior of the error defined in (40) for $a\ell = \ln(1/h)$ is presented in Table 3. This choice of a and choosing $N = nz = 1/h$, yields the rate

TABLE 3

Observed errors $\|u - w_{h,N}^{a,\ell}\|$ between finite element reference solution with standard boundary condition and the solution $w_{h,N}^{a,\ell}$ based on the PML approach with parameters $a = \ln(1/h)/\ell$ and $\ell = 0.1$ measured in the norm defined in (40).

		N				
nz	a	51	101	201	401	801
64	44.36	0.0277	0.0264	0.0263	0.0263	0.0263
128	47.77	0.0143	0.0118	0.0116	0.0116	0.0116
256	54.60	0.0098	0.0060	0.0056	0.0055	0.0055
512	62.63	0.0082	0.0034	0.0029	0.0028	0.0027
1024	69.59	0.0076	0.0022	0.0016	0.0014	0.0013

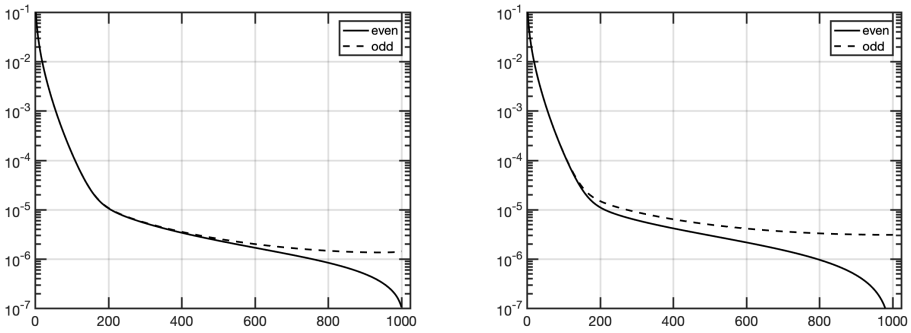

FIG. 3. *Decay of the norms $\|u_n\|_{L^2(0,1)}$ (left) and $\|w_n^{\ell,a}\|_{L^2(-\ell,1+\ell)}$ (right) of the moments for the two numerical solutions with standard and PML boundary condition and layer parameters $a = 30$ and $\ell = 0.1$.*

$O(h)$. The previous computations suggest that the assumptions of Remark 19 are reasonable for our example.

Let us briefly comment on the smoothness of the solutions u and $w^{\ell,a}$ for the model with standard and PML boundary conditions. In Figure 3, we visualize the decay of the moments u_n and w_n in the corresponding spherical harmonics expansions for the two reference solutions u and $w^{\ell,a}$ computed on the finest grid with $N = 1001$ moments and $nz = 1024$ elements. Let us note that the decay of the moments is very similar for both variants of the boundary conditions, and one can therefore expect a very similar convergence behavior with $N \to \infty$. Let us also note that the decay of the moments slows down for large N. This can be explained by a lack of smoothness of the solution close to the boundary, which is due to the homogeneous inflow boundary conditions, i.e., the discontinuity of $\mu \mapsto u(0,\mu)$ for $\mu = 0$.

Let us close this section by verifying numerically the efficiency of the PML approach, which we indicate in section 6.4. Let

$$u(z,\mu) = \sin(\pi z)\chi_{(0,1)}(\mu) \tag{41}$$

with $\chi_{(0,1)}$ being the characteristic function of the interval $(0,1)$. We choose σ and σ_s as above and define $q(z,\mu)$ such that $u(z,\mu)$ is the exact solution to the radiative transfer equation (38). Due to the nonsmoothness of u with respect to μ, we expect that N needs to be large in order to obtain a good approximation. Table 4 shows

TABLE 4

Observed errors between the exact solution u defined in (41) and the finite element solution $u_{h,N}$ with standard boundary condition and the solution $w^{a,\ell}_{h,N}$ based on the PML approach with parameters $a = 10$, $\ell = 0.1$ and $nz = 128$ measured in the norm defined in (40). The solution is obtained after k CG iterations with tolerance 10^{-5} in t seconds CPU time.

	Standard			PML		
N	$\|u - u_{h,N}\|$	t	k	$\|u - w^{a,\ell}_{h,N}\|$	t	k
511	0.0176	1.74	1614	0.0176	1.73	1608
1023	0.0125	4.42	1647	0.0125	3.60	1634
2047	0.0089	12.98	1684	0.0089	7.44	1650
4095	0.0066	49.79	1697	0.0066	15.70	1650

the errors as well as the computation times for the standard approach and the PML approach. We observe a convergence of the error of order $1/\sqrt{N}$ for both methods, which fits to the regularity of u. The errors for both approaches are almost identical. As already observed in Table 3, the PML treatment of the boundary conditions again introduces only a minor perturbation. A similar reasoning as in section 6.4 shows that the memory complexity and the computational complexity of matrix-vector multiplications for the standard approach is $O(h^{-1}N^2)$, while the corresponding complexities for the PML approach are $O(h^{-1}N)$; i.e., the expected runtimes for the PML approach grow linearly in N, while for the standard approach the runtime grows quadratically in N. These theoretical estimates are verified by the computations shown in Table 4. In addition, we observe that the conjugate gradient method requires almost the same number of iterations for the corresponding approaches, which indicates that the conditioning of both systems is similar, and thus the enhanced complexity of matrix-vector multiplications in the PML approach directly translate into an enhanced performance of the overall solution process.

7.2. Checkerboard test. The potential of the proposed method to solve large-scale problems is illustrated by computational experiments for a lattice problem, which is used as a test case for simulating the core of a nuclear reactor in the nuclear engineering communities. The geometric setup of the problem, the absorption, and the scattering parameters are depicted in Figure 4. The source is defined as $q(r, s) = 1$ for $3 \le r_1, r_2 \le 4$, $s \in \mathcal{S}$ and $q(r, s) = 0$ else. Since the coefficient functions and the

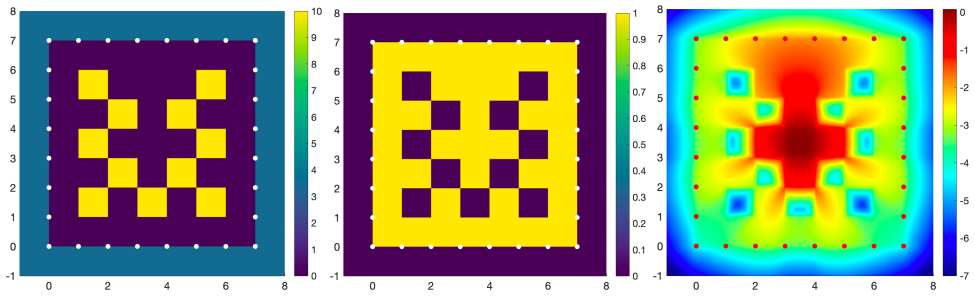

FIG. 4. *Sketch of the computational setup. Left: Extended absorption parameter with $e^{-a\ell} = 1/32$ on $\mathcal{R}^\ell \setminus \mathcal{R}$. Middle: Extended scattering coefficient on $\mathcal{R}^\ell$. The domain $\mathcal{R}$ is enclosed by the dotted line. Right: $\log_{10}$-plot of the angular average of the reference solution.*

TABLE 5

Observed errors between the finite element solutions computed on the reference grid for different layer parameters a with norm defined in (42).

$e^{-a\ell}$	1/2	1/4	1/8	1/16
$\|w_{h,N} - w_{h,N}^{\ell,a}\|$	0.00146	0.00068	0.00035	0.00014

source term have jump discontinuities, we expect that good numerical approximations require large N. In this case, the implementation of inflow boundary conditions using half-space integrals (4) is not practical; refer to section 7.3 for an in-depth discussion. Therefore, we confine ourselves to show exponential decay of the error in terms of the layer parameter $a\ell$ and that our method can be used to compute high-order P_N-approximations efficiently.

We compute a reference solution $w_{h,N} = w_{h,N}^{\ell,a}$ for $e^{-a\ell} = 1/32$ on a grid with 332 929 vertices, 663 552 triangles, and spherical harmonics of order $N = 31$, i.e., 1 024 Fourier coefficients; see Figure 4 for a plot of the mean of the reference solution. The number of degrees of freedom for approximating the solution is 515 488 240, which amounts to nearly 4GB of memory to just store the even and odd parts of the solution. For the even part we have 165 132 784 degrees of freedom. Table 5 shows the error

$$\left(\left\| w_{h,N} - w_{h,N}^{a,\ell} \right\|_{L^2(\mathcal{D})}^2 + \left\| s \cdot \nabla \left(w_{h,N}^{+} - w_{h}^{a,\ell,+} \right) \right\|_{L^2(\mathcal{D})}^2 \right)^{1/2} \tag{42}$$

of the finite element approximation computed on the same grid but for different damping parameters a to the reference solution. As predicted by theory, the error decays exponentially. Regarding the efficiency of the numerical solver, we have observed that the number of PCG iterations only slightly increases with N but is robust in $a\ell$. More precisely, the number of PCG iterations decreased from 270 for $e^{-a\ell} = 1/2$ to 226 for $e^{-a\ell} = 1/32$. We observed this favorable behavior, which can be explained by the fact that the numerical solution is close to zero in the absorbing layer, in several other numerical tests as well.

7.3. Fully three-dimensional problem. For three-dimensional problems the approximation of inflow boundary conditions with P_N-methods leads to large-scale computations. Since the matrices `B`, `C`, and `M` exhibit a tensor product structure, they can be stored efficiently. This is, however, not the case for the matrices that arise from the discretization of the half-space integrals (4), which introduce a coupling of all spherical harmonics. In order to illustrate this issue, we provide in Table 6 the memory requirements of the matrices of the corresponding boundary functionals, where we used a workstation with 16GB of memory. As a computational domain we have chosen the unit ball in $\mathbb{R}^3$. We clearly see the quadratic growth in terms of memory with respect to the spatial mesh size h as well as the growth to fourth order in the order of the spherical harmonics N; i.e., the memory requirements for the boundary terms are of the order $h^{-2}N^4$. This growth, in terms of N, makes P_N-methods with the standard implementation of inflow boundary conditions prohibitive for computations in fully three-dimensional geometries if the problem admits solutions with a nontrivial dependence on s. As estimated in section 6.4, the memory requirements for the PML approach are $O(h^{-3}N^2)$, cf. Table 6, while the standard approach requires $O(h^{-3}N^2 + h^{-2}N^4)$ memory. Thus, if $N \geq \sqrt{1/h}$ is required for an accurate approximation of the exact solution, the PML approach has better computational complexity than

TABLE 6

Memory requirements for the matrices approximating the inflow boundary conditions via discretization of half-space integrals (top), where oom means out of memory, and the same for the fully assembled boundary functional of the PML approach (bottom), which could be reduced to 620kB if the tensor product structure were used.

	N				
h	9	11	13	15	17
0.12	70MB	151MB	287MB	500MB	812MB
0.06	282MB	605MB	1.12GB	1.95GB	3.17GB
0.03	1.11GB	2.37GB	4.5GB	oom	
0.12	1MB	2MB	3MB	3MB	4MB
0.06	6MB	8MB	11MB	15MB	19MB
0.03	27MB	40MB	55MB	73MB	93MB

the standard approach, because matrix-vector multiplications can be performed with optimal complexity in our PML approach. Note that Table 3 indicates that a choice $N \sim 1/h$, or, in view of Table 4, even $N \sim 1/h^2$, seems to be an adequate choice if the overall error should be $O(h)$. Thus, using the PML approach, it is attractive to employ iterative solvers, such as the PCG method that we used above.

8. Discussion and further applications. We have presented a PML approach for the efficient treatment of vacuum boundary conditions in radiative transfer. The choice of reflection boundary condition on the boundary of the extended domain was specifically tailored to obtain a mixed variational formulation that leads to sparse linear systems and can be implemented easily. The theory is supported by extensive numerical simulations (i) verifying the predicted convergence and (ii) showing the superiority in terms of memory requirements compared to the standard approximation using half-space integrals. These low memory requirements are key for large scale computation in three-dimensional problems. In view of our detailed error estimates, it seems possible to analyze different artificial boundary conditions for the extended problem as well. As mentioned in the introduction, a relevant case is periodic boundary conditions, which in turn can be used to develop pseudospectral methods; see [18]. Besides different boundary conditions it seems possible to generalize our results to nonconstant extensions of the absorption coefficient as long as sufficient decay of the solution within the absorbing layer is guaranteed. Finally, let us briefly comment on a further possible application of the theory.

Least-squares formulations. A powerful method for the solution of first order equations is the least-squares approach that has been developed for the radiative transfer equation in [15] and has been widely used [12, 21]. The basic approach is to minimize the functional

$$\|s \cdot \nabla u + \mathcal{C}u - q\|^2_{L^2(\mathcal{D})} + \|u\|^2_{L^2(\partial\mathcal{D}_-;|s\cdot n|)}$$

in the space $\mathcal{W}^2 = \{v \in W^2(\mathcal{D}) : v_{|\partial\mathcal{D}_-} \in L^2(\partial\mathcal{D}_-; |s\cdot n|)\}$. Here, the homogeneous inflow boundary conditions are approximated by incorporating the boundary functional $\|u\|_{L^2(\partial\mathcal{D}_-;|s\cdot n|)}$. As mentioned in the introduction, the numerical approximation of such half-space integrals makes the numerical realization of the minimization problem difficult. Based on the approach of this paper, it is natural to investigate minimization of the functional

$$\left\|s\cdot\nabla\bar{w}^{\ell,a}+\mathcal{C}^{\ell,a}\bar{w}^{\ell,a}-q^{\ell}\right\|^2_{L^2(\mathcal{D}^\ell)}+\left\|\bar{w}^{\ell,a}\right\|^2_{L^2(\partial\mathcal{D}^\ell)}$$

in the space $\mathcal{W}^\ell = \{v \in W^2(\mathcal{D}^\ell) : v_{|\partial\mathcal{D}^\ell} \in L^2(\partial\mathcal{D}^\ell)\}$. This is currently under investigation by the authors.

REFERENCES

[1] V. Agoshkov, *Boundary Value Problems for Transport Equations*, Model. Simul. Sci. Eng. Technol, Birkhäuser, Boston, 1998.

[2] S. Arridge, H. Egger, and M. Schlottbom, *Preconditioning of complex symmetric linear systems with applications in optical tomography*, Appl. Numer. Math., 74 (2013), pp. 35–48.

[3] S. R. Arridge, *Optical tomography in medical imaging*, Inverse Problems, 15 (1999), pp. R41–R93, https://doi.org/10.1088/0266-5611/15/2/022.

[4] J.-P. Berenger, *A perfectly matched layer for the absorption of electromagnetic waves*, J. Comput. Phys., 114 (1994), pp. 185–200, https://doi.org/10.1006/jcph.1994.1159.

[5] K. M. Case and P. F. Zweifel, *Linear Transport Theory*, Addison-Wesley, Reading, MA, 1967.

[6] S. Chandrasekhar, *Radiative Transfer*, Dover Publications, Inc., NY, 1960.

[7] B. Chang and B. Lee, *A multigrid algorithm for solving the multi-group, anisotropic scattering Boltzmann equation using first-order system least-squares methodology*, Electron. Trans. Numer. Anal., 15 (2003), pp. 132–151.

[8] R. Dautray and J. L. Lions, *Mathematical Analysis and Numerical Methods for Science and Technology. vol.* 6*, Evolution Problems* II, Springer, Berlin, 1993.

[9] J. J. Duderstadt and W. R. Martin, *Transport Theory*, John Wiley & Sons, Inc., New York, 1979.

[10] H. Egger and M. Schlottbom, *A mixed variational framework for the radiative transfer equation*, Math. Models Methods Appl. Sci., 22 (2012), 1150014.

[11] H. Egger and M. Schlottbom, *An L^p theory for stationary radiative transfer*, Appl. Anal., 93 (2014), pp. 1283–1296, https://doi.org/10.1080/00036811.2013.826798.

[12] K. Grella and C. Schwab, *Sparse tensor spherical harmonics approximation in radiative transfer*, J. Comput. Phys., 230 (2011), pp. 8452–8473, https://doi.org/10.1016/j.jcp.2011.07.028.

[13] T. Hagstrom, *Radiation boundary conditions for the numerical simulation of waves*, Acta Numer., 8(1999) pp. 47–106, https://doi.org/10.1017/S0962492900002890.

[14] E. E. Lewis and W. F. Miller, Jr., *Computational Methods of Neutron Transport*, John Wiley & Sons, Inc., New York, 1984.

[15] T. A. Manteuffel, K. J. Ressel, and G. Starke, *A boundary functional for the least-squares finite-element solution for neutron transport problems*, SIAM J. Numer. Anal., 37 (2000), pp. 556–586.

[16] G. I. Marchuk and V. I. Lebedev, *Numerical Methods in the Theory of Neutron Transport*, Harwood Academic Publishers, Chur, Switzerland, 1986.

[17] M. F. Modest, *Radiative Heat Transfer*, 2nd ed., Academic Press, New York, 2003.

[18] S. Powell, B. T. Cox, and S. R. Arridge, *A pseudospectral method for solution of the radiative transport equation*, J. Comput. Phys., 384(2019), pp. 376–382

[19] J. Tervo and P. Kolmonen, *Inverse radiotherapy treatment planning model applying Boltzmann-transport equation*, Math. Models Methods Appl. Sci., 12 (2002), pp. 109–141, https://doi.org/10.1142/S021820250200157X.

[20] V. S. Vladimirov, *Mathematical problems in the one-velocity theory of particle transport*, tech. report, Atomic Energy of Canada Ltd. AECL-1661, 1963 (in English); Tr. Mat. Inst. Steklova, 61(1961) (in Russian).

[21] G. Widmer, R. Hiptmair, and C. Schwab, *Sparse adaptive finite elements for radiative transfer*, J. Comput. Phys., 227 (2008), pp. 6071–6105.

[22] S. Wright, S. R. Arridge, and M. Schweiger, *A finite element method for the even-parity radiative transfer equation using the P_N approximation*, in Numerical Methods in Multidimensional Radiative Transfer, G. Kanschat, E. Meinköhn, R. Rannacher, and R. Wehrse, eds., Springer-Verlag, Berlin, 2009.